TOPICAL REVIEW • OPEN ACCESS

The properties of solids: ‘If you want to understand function, study structure’

OPEN ACCESS
IOP Publishing
Journal of Physics: Condensed Matter
J. Phys.: Condens. Matter **37** (2025) 113001 (11pp)
https://doi.org/10.1088/1361-648X/ada412

Topical Review

The properties of solids: 'If you want to understand function, study structure'

R O Jones

Peter-Grünberg-Institut PGI-1, Forschungszentrum Jülich, D-52425 Jülich, Germany

E-mail: r.jones@fz-juelich.de

Received 15 August 2024, revised 9 December 2024
Accepted for publication 30 December 2024
Published 9 January 2025

Abstract

The importance of the structure-function relationship in molecular biology was confirmed dramatically by the recent award of the 2024 Nobel Prize in Chemistry 'for computational protein design' and 'for protein structure prediction'. The relationship is also important in chemistry and condensed matter physics, and we survey here structural concepts that have been developed over the past century, particularly in chemistry. As an example we take structural phase transitions in phase-change materials (PCM), which can be switched rapidly and reversibly between amorphous and crystalline states. Alloys of Ge, Sb, and Te are the materials of choice for PCM optical memory; they satisfy practical demands of stability and rapid crystallization, which results in metastable, rock salt structures, not the most stable (layered) crystalline forms.

Keywords: structure/function relationship, factors determining structures of molecules and solids, phase-change materials, alloys of Ge, Sb, Te

1. Introduction

It is not surprising that the statement of Francis Crick: 'If you want to understand function, study structure' [1, p 150] is from his 'molecular biology days'; the folding of a random coil of amino acids to a biologically active protein is just one example of the central role played by 'structure' in that field. The importance of this relationship was emphasized by the recent award of the 2024 Nobel Prize in Chemistry to David Baker 'for computational protein design' and to Demis Hassabis and John Jumper 'for protein structure prediction.' In the latter case, artificial intelligence algorithms were used to predict the structure of proteins, based solely on their amino acid sequences. The manifold applications cited by the Nobel Prize committee include 'proteins that can be used as pharmaceuticals, vaccines, …' and 'understanding antibiotic resistance and creating images of enzymes that can decompose plastics' [2].

The atomic arrangement of molecules and solids, however, is also the focus of much of chemistry and is an essential part of condensed matter physics. The extended title of Linus Pauling's iconic textbook 'The Nature of the Chemical Bond and the Structure of Molecules and Crystals' [3] shows the focus on structural properties that characterized the career of one of the most famous chemists. His doctoral work covered x-ray diffraction (XRD) studies of compounds including molybdenite MoS_2 and barite $BaSO_4$, and this led to the development of 'rules' determining the structure of ionic crystals [4]. It was inevitable that crystallographers have sought the best

ways to catalog '... some seven hundred different structure types found in metals and alloys' [5, p viii], with impressive results.

The wide-ranging survey of crystal structures by Pearson [5] listed numerous factors affecting crystal structure, including geometrical factors such as space-filling, the sizes and electronegativities of the component atoms, and the electronic band structures of the materials. These factors play different roles in different families of materials, although the close relationships between factors such as atomic sizes and electronegativities can make them difficult to entangle. Nevertheless, the electrostatic forces in ionic crystals are relatively simple to treat, and the spherical nature of electron distributions of rare-gas configurations allows one to focus on the relative sizes of the ions [3, chapter 13], [4, 6]. Metallurgists are interested in the structures of metals, their alloys, and their mixtures, where both packing considerations and electronic structure play important roles. The importance of the latter was evident already in the early work of Hume-Rothery (e.g. [7, 8]), who showed that some alloy structures occur at definite electron/atom ratios, e.g. the β-structure with 21 valence electrons to 13 atoms. The directional bonds found in covalently bonded materials have focused attention on electronic structure, particularly in semiconductors.

This 'topical review' focuses on the geometrical arrangement of the atoms in materials and molecules and follows two earlier reviews that are summarized in [9]: The history of chemical bonding was surveyed in [10], from the first use of the term 'bond' by Frankland in 1866 [11, 12]; the second [13] extended the discussion to aspects of bonding that have become important recently in the phase change materials (PCM) context. The 'review' part of the present article focuses on concepts that are valuable in a wide range of contexts, particularly in chemistry. In section 2, we discuss the characterization of structures in ionic solids, metals and their alloys, and semiconductors, including structural instabilities (particularly 'Peierls' distortions). Extended discussions of crystalline solid state structures are given in Pauling [3, chapter 13], Pearson [5], and Müller [14]; Burdett [15, chapters 6–8] and Berger *et al* [16] emphasize the importance of connecting the viewpoints of chemists and physicists on these problems.

The 'topical' aspect of the present article focuses on PCM, where the reversible *structural* transition between the crystalline and amorphous phases of nanosized bits in a polycrystalline layer results in dramatic property changes. The pronounced difference between the optical reflectivity or resistivity is often used to identify the phase. The (nanosecond) speed of crystallization of the amorphous phase is the basis of digital versatile discs and Blu-ray Disc rewritable optical memory, and the importance of 'structure' in such a transition is clear. The materials with favourable properties are often narrow-gap semiconductors comprising a small number of heavy main-group elements, particularly Sb and Te. The search for improved PCM has also invoked other properties of materials, including the nature of their chemical bonds [17, and references therein] [18, 19]. The structures of PCM (section 3) are discussed in section 4, which is followed by concluding remarks (section 5).

2. Structure

The discovery of XRD over a century ago led to a rapidly expanding database of crystal structures that provided a challenge to understand their patterns and to develop 'rules' for predicting unknown structures. We begin with ionic crystals.

2.1. Geometrical considerations, ionic crystals

The relative simplicity of Coulomb interactions in ionic crystals and the spherical symmetry of ions with noble gas electronic configurations make them attractive objects for study. This leads naturally to arguments based on the packing of spheres[1].

Goldschmidt [6, 21] was the first to provide general 'rules' concerning the relationship between chemical composition and crystal form. His first rule is that the crystal structure is determined by the size ('Größe') and polarizability of the components, which are understood to be atoms, ions, and groups of both. The 'size' depends naturally on the atomic number, charge, etc and further rules discussed the trends to be expected. The first works of Pauling on the structure and properties of ionic crystals [22, 23] used the 'sizes of ions' in the title, and the first of his principles determining the structure of complex ionic crystals focused again on the 'size' (or radii) of the constituents [4]. If a coordinated polyhedron of anions is formed about each cation, the cation-anion distance is determined by the *sum* of their radii and the coordination number of the cation by the *ratio* of the cation radius r_+ to the anion radius r_- [3, chapter 13]. Geometric considerations led Pauling to propose the existence of critical ratios that separate eight- from sixfold coordination ($\sqrt{3}-1=0.732$) and six- from fourfold coordination ($\sqrt{2}-1=0.414$).

Effective ionic radii determined, for example, by Zachariasen [24], Ladd [25], or Shannon and Prewitt [26, 27] have proved to be useful in rationalizing and predicting crystal structures, but Burdett noted that the second part of the above rule is not particularly successful. If the structures of AB octet materials are plotted against r_+ and r_- (one of many possible 'structure maps'), the boundaries between different structure types are not consistent with these critical values [15, p 195], although a similar plot for A_2BO_4 structures leads to boundaries in good agreement with experiment. A more recent statistical study of more than 5000 oxide structures provides an even more sobering assessment [28]. The first rule is satisfied in only 66% of the structures analyzed, and only 13% satisfy simultaneously the remaining four rules, 'indicating a much lower predictive power than expected' [28].

2.2. Laves phases and principles

In his 1930 dissertation [29, 30], Fritz Laves presented a classification of crystal structures based on topological concepts,

[1] Sphere packing considerations are not necessarily simple. The Kepler conjecture of 1611, that the densest packing of identical spheres has a face-centred-cubic structure, was not proven until 1998. See [20] for a readable account of packing problems.

and Laves and Witte [31] proposed a geometrical principle for understanding the structures of the magnesium-based alloys $MgNi_2$, $MgCu_2$, and $MgZn_2$ of the form AB_2 ('Laves phase'). In these alloys, two kinds of spherical atoms with radius ratio of 1.2:1 can be closely packed to form polyhedra with unusually high coordination numbers. Laves and Witte [32] subsequently suggested that the differences between the structures might be related to differences in the number of valence electrons per atom, the valence electron concentration (VEC).

Laves phases are intermetallic phases with composition AB_2 and are classified on the basis of geometry alone, namely the packing of spheres of two different sizes. In general, the A atoms are ordered as in diamond, hexagonal diamond, or a related structure, and the B atoms form tetrahedra around the A atoms. If the two types of atoms are perfect spheres with a size ratio of $\sqrt{3/2} = 1.225$, the structure would be topologically tetrahedrally close-packed. At this size ratio, the structure has an overall packing volume density of 0.710 [33]. The atomic radii used in intermetallic compounds are discussed in [34], and a recent and very extensive review of Laves phases can be found in [35]. Electronic structure calculations [36] indicate that the bonding is determined by the difference in electronegativity between A and B. If this is small, the bonding is multicentre in nature; much larger values lead to large charge transfer and the formation of polyanions of B_2.

The structures of simple ionic compounds are governed by the principles of Laves [37]: dense packing, high coordination, and high symmetry resulting from the non-directional character of the interactions, as well as finding a favourable balance of electrostatic forces between the ions. While these general principles guide structure-building, the structures adopted in specific cases depend on the relative sizes of cations and anions, and anion-anion repulsions must be avoided inside anion coordination polyhedra. The rules may be summarized as follows: (1) the ratio of the radii of cations and anions and the stoichiometric proportions of the components MX, MX_2 determine the maximum number of anions in the coordination polyhedra around the cations. (2) symmetry and packing considerations lead to choice of the most symmetrical coordination polyhedra possible. These conditions mean that simple ionic compounds (MX, MX_2) are accommodated in a relatively small number of different crystal structural types.

The space-filling arguments of Laves were extended by Parthé [38], who introduced the radius ratio and showed that space-filling could be expressed in a form that is independent of the size of the atoms involved, but is characteristic of the structure type. On the basis of these arguments, Parthé predicted correctly that pressure on the orthorhombic structure of black phosphorus would lead to a rhombohedral (A7) structure [38]. Nevertheless, the assumption of rigid atoms of fixed size limits the applicability of this approach.

2.3. Zintl–Klemm concept

Zintl phases [39] are compounds comprising a metallic element from groups 1 (alkali) or 2 (alkaline earths) and an element of groups 13–16. They are characterized by bonding intermediate between ionic and metallic; group 13 elements usually lead to intermetallic compounds, while elements with larger electronegativity in groups 14–16 lead to ionic (salt-like) solids [40]. The demarcation between groups 13 and 14 is often referred to as the 'Zintl line' or 'Zintl border' [40]. The structures of the ionic phases involve electron transfer from the metal to the more electronegative main-group element. The latter form a 'polyanion' structure similar to that of clusters of the isovalent element [41]. Many examples are shown in [42], and the mechanism is often referred to as the 'Zintl–Klemm concept' [43]. The focus is generally on electron transfer to satisfy the Lewis octet rule (each main-group atom shares eight electrons with its neighbours), but the concept can be extended to electron-rich ('hypervalent') networks that do not satisfy this rule [44].

2.4. Electron counting in reciprocal space: Hume-Rothery, Mott and Jones

The experimental work of Hume-Rothery starting in 1926 [7] [8, p 196] showed that certain crystal structures exist for a narrow range of electron concentrations for various compositions of elements of similar size; Well-studied examples are Cu–Zn alloys (brasses). Mott and Jones [45, p 170 ff], [46, 47] argued that structures will be favoured for electron concentrations where the Fermi surface crosses the first Brillouin zone, in the case of Cu–Zn alloys, or larger zones in systems with higher electron concentrations. There have been numerous refinements of this picture in the intervening 90 years, including the rapid variation in the dielectric function near the Fermi energy [48, and references therein] and detailed band structure calculations including d-electrons [49]. Nevertheless, the basic principles, electron counting in perturbed free-electron bands and the corresponding densities of states, have 'been repeatedly affirmed' [16]. 'The basic idea of Mott and Jones is correct. Structural stability of similarly packed phases *is* largely determined by the density of states. . . .This is in turn dominated by the structure of the Brillouin zone.' [49]. A recent computational study of many (cubic) ordered binary compounds involving a range of bonding mechanisms and including transition and rare earth elements concluded that 'we consider the physics behind the Hume-Rothery electron concentration rule to be well established' [50]. It is inevitable that structures with very complex Brillouin zones complicate the application of these rules, and Pearson [5, pp 80–83] emphasizes that the electron concentration is not the only energy band factor that can influence crystal structure.

2.5. Metals

The lack of coordination or valence restrictions in metallic phases leads to many types of structure, and it is difficult to find a single simple system of classifying the structures of all metallic phases [5]. Metallic elements usually have close-packed [face-centred cubic (FCC) or hexagonal close-packed] or body-centred cubic (BCC) structures. The first two have 12 nearest neighbours, and BCC structures have eight nearest neighbours with six next-nearest neighbours

only 15.5% farther away[2]. The large number of neighbours in metals is often associated with the close packing of spheres. This argument is more convincing for the group 1 (alkali) and group 2 (alkaline earth) metals with s (and no p) valence electrons than in other elements.

Interest in using 'structure maps' to understand the relationship between composition and the crystal structures of binary compounds $A_{1-x}B_x$ with the same stoichiometry goes back at least 90 years [52]. These maps seek suitable coordinates that result in a clear separation of alloys of known structure into regions separated from those of other structures (see, for example, [53]). These coordinates involve physical properties that could be relevant to structural stability, including electronegativities [54, 55], valence orbital radii [56], and the number of valence electrons [57]. A remarkably simple, phenomenological scheme was provided by Pettifor [58], who assigned a single number to each element, so that the structures of AB alloys could be presented in a single two-dimensional array. These numbers provided very good structural separation of hundreds of AB compounds, and the use of such structure maps to find intermetallic compounds with required structure and mechanical properties is discussed in [59]. It is a separate challenge to develop computational methods to provide input data that are not available experimentally.

2.6. Semiconductors, semimetals

In 1959, Mooser and Pearson [60] noted that the relationships between chemical composition and crystal structures had largely been restricted to metals and alloys or to ionic materials, and they sought a structure map that applies to compounds of the form A_iX_j $(i,j = 1-3)$, including many semiconductors. There are well-known variations in properties and structures with increasing principal quantum number; in group 14, for example, C is an insulator, Si and Ge are semiconductors, Sn is stable as a metal or as a semiconductor, and Pb is a metal; in group 16, the structures are helical chains that come progressively closer in the sequence S $\longrightarrow$ Se $\longrightarrow$ Te $\longrightarrow$ Po, the last of which is simple cubic (SC). For the axes on their structure maps, Mooser and Person [60] took the mean of the principal quantum numbers of the constituent atoms $\bar{n}$ and the difference between the arithmetic means of the electronegativities of the anions and cations. The maps showed a striking separation of AX compounds into groups with different crystal structures and the separation of AX_2, AX_3, and A_2X_3 structures into groups with different packing densities.

Elements in the main groups 14–16 are mainly semiconductors or semimetals, and this is often true when they are components of binary and ternary compounds. The valence electrons of these elements have s- and p-character and are often discussed using perturbation theory of free-electron band structures (including the nearly free-electron (NFE) model [61] and pseudopotentials [10, section 4.2]).

2.7. Structures in materials with average valence five, $\langle \mathbf{5} \rangle$

The NFE model was used 90 years ago by Jones [62] to study the structure and properties of bismuth, whose valence configuration ($6s^26p^3$) has a half-filled p-shell. Jones showed that a zone could be constructed in reciprocal space that was bounded by planes with prominent Bragg reflections (large structure factors) and contained 10 electrons (two atoms with five electrons each in the unit cell). He showed that a SC (metallic) form of Bi would be unstable against a distortion to the rhombohedral (A7) structure that is the most stable crystalline form of Bi, and the low (semimetallic) conductivity and large diamagnetism could be explained in simple NFE terms. Details are given elsewhere [10, 13, 63]. It is remarkable that this symmetry-breaking argument in a three-dimensional system is generally referred to as a 'Peierls distortion', after the one-dimensional model introduced over 20 years later [64][3]. The 'Jones zone' for the diamond structure provided the basis of a model calculation of the optical properties and charge distributions in Si and Ge [67], and its role in determining the same quantities in materials with an *average* [denoted by $\langle \ldots . \rangle$] of five valence electrons [$\langle \mathbf{5} \rangle$: As, Sb, Bi, PbS, PbSe, PbTe, SnTe, GeTe] is discussed in [68]. The relatively simple forms of the Jones zone [63, figures 7(b) and (d)] in both families of materials is consistent with the existence of a single dominant peak in the optical spectra in all cases [67, 68].

Cohen *et al* [69] examined the structures (electronic and geometric) of $\langle \mathbf{5} \rangle$-systems: the elemental semimetals As, Sb, and Bi (A7 structure) and semiconductors SnTe, PbS, PbSe, PbTe (rock salt structures). $Ge_{1-x}Sn_xTe$ alloys form a continuous range of solid solutions, changing from rock salt to A7 structure at temperatures that decrease with increasing Sn content [70] from 700 K in GeTe. 'The SC structure is apparently stabilized by the chemical difference between the 14 and 16 components' [69]. Cohen *et al* emphasize, however, the small difference between the A7 and rock salt structures. They also noted the structural regularities for average valence four, $\langle \mathbf{4} \rangle$: elements of group 14, many 13–15 compounds, and some 12–16 compounds. The diamond structure is favoured in the first, in the others either the zinc blende structure or a hexagonal analogue. These structures all involve tetrahedral coordination of the nearest neighbours, in contrast to the octahedral coordination prevalent in $\langle \mathbf{5} \rangle$-systems, where the contribution of s-electrons to bonding is smaller [69].

2.8. Property trends

Insight into trends in structures and properties of elements and compounds can be found by discussing them in terms of appropriate variables (coordinates). Cohen *et al* [69] focus on the Fourier components of the pseudopotential, particularly those in the 14–16 group semiconductors and semimetals that are antisymmetric about the midpoint between the two

[2] R Hoppe suggests an 'effective coordination number' of 9.6 for the BCC structure [51, p 29].

[3] Friedel does refer to 'Hume-Rothery-Jones phases' [65], and Shick *et al* describe the metal-semimetal transition in Bi as a 'Jones-Peierls-type transition' [66].

Table 1. Moments $\langle r\rangle_0$ and $\langle r\rangle_1$ (Å), and the density functional (Kohn–Sham) eigenvalues ε_0 and ε_1 (hartree) for *s*- and *p* valence orbitals of atoms of groups 13–17.

Group	Element	$\langle r\rangle_0$	$\langle r\rangle_1$	ε_0	ε_1
	B	1.033	1.218	−0.347	−0.133
	Al	1.346	1.824	−0.285	−0.100
13	Ga	1.240	1.812	−0.329	−0.095
	In	1.381	1.980	−0.302	−0.093
	Tl	1.311	2.039	−0.351	−0.087
	C	0.832	0.953	−0.506	−0.194
	Si	1.145	1.479	−0.398	−0.150
14	Ge	1.120	1.534	−0.431	−0.143
	Sn	1.265	1.728	−0.385	−0.132
	Pb	1.223	1.787	−0.443	−0.129
	N	0.698	0.786	−0.686	−0.264
	P	1.003	1.256	−0.514	−0.203
15	As	1.026	1.352	−0.533	−0.191
	Sb	1.178	1.545	−0.472	−0.178
	Bi	1.150	1.619	−0.532	−0.168
	O	0.603	0.670	−0.881	−0.332
	S	0.897	1.096	−0.634	−0.258
16	Se	0.950	1.219	−0.635	−0.240
	Te	1.104	1.414	−0.553	−0.219
	Po	1.088	1.494	−0.622	−0.207
	F	0.531	0.585	−1.099	−0.408
	Cl	0.813	0.976	−0.760	−0.316
17	Br	0.886	1.114	−0.740	−0.289
	I	1.040	1.310	−0.640	−0.261
	At	1.034	1.394	−0.712	−0.245

FCC sublattices in the rock salt structure. Large antisymmetric components lead to insulating behaviour, as in NaCl. Other examples [53, 63] include the atomic valence orbitals and the electronegativities of the component atoms (and their differences).

It has proved useful in this context to characterize the valence orbitals of atoms by their Kohn–Sham eigenvalues from density functional calculations or by their radial moments, the normalized expectation values of r with respect to the orbitals R_{nl}:

$$\langle r\rangle_{nl} = \int \mathrm{d}r\, r\, |rR_{nl}|^2 \Big/ \int \mathrm{d}r\, |rR_{nl}|^2 \,. \qquad (1)$$

Here n and l are the principal and angular momentum quantum numbers, respectively. The radial moments probe an orbital over its entire range and is a measure of its 'size'. The Kohn–Sham eigenvalues and the radial moments for s- and p-valence orbitals of elements of groups 13 to 17 are given in table 1 and in figures 1 and 2.

Both the moments and the eigenvalues reflect the zig-zag behaviour in the properties of elements in a column of the periodic table with increasing atomic number [63, and references therein]. 'Secondary periodicity' has been known for more than a century [71] and is a consequence of the 'd-block' and 'lanthanide' contractions in valence orbitals occurring when 3d- and 4f-electrons, respectively, are first present in the core. Clearly evident in the plots of both moments and eigenvalues is the relativistic contraction of the valence s-orbitals, particularly in heavy elements (principal quantum number 6). This leads to weaker s-p hybridization and stabilization of lower oxidation states as the atomic number increases.

Pauling [3, 72] defined electronegativity in terms of the bond energies of small molecules, while Mulliken defined an 'absolute' electronegativity as the average of ionization energy and electron affinity of individual *atoms* [73]. The Kohn–Sham eigenvalues and orbital moments discussed here follow the spirit of the latter. A classical density functional study of simple binary alloys of hard spheres showed that relative atomic sizes are crucial in determining the crystal structures [74], in particular the linear lattice constant-concentration relationship known empirically as 'Vegard's Law' [75]. This suggests that average moments ('sizes') can be tuned by alloying, e.g. by replacing Ge by Si in a solid solution.

3. Phase change materials

The choice of practical PCM rests on several essential criteria. Thin films of the material must:

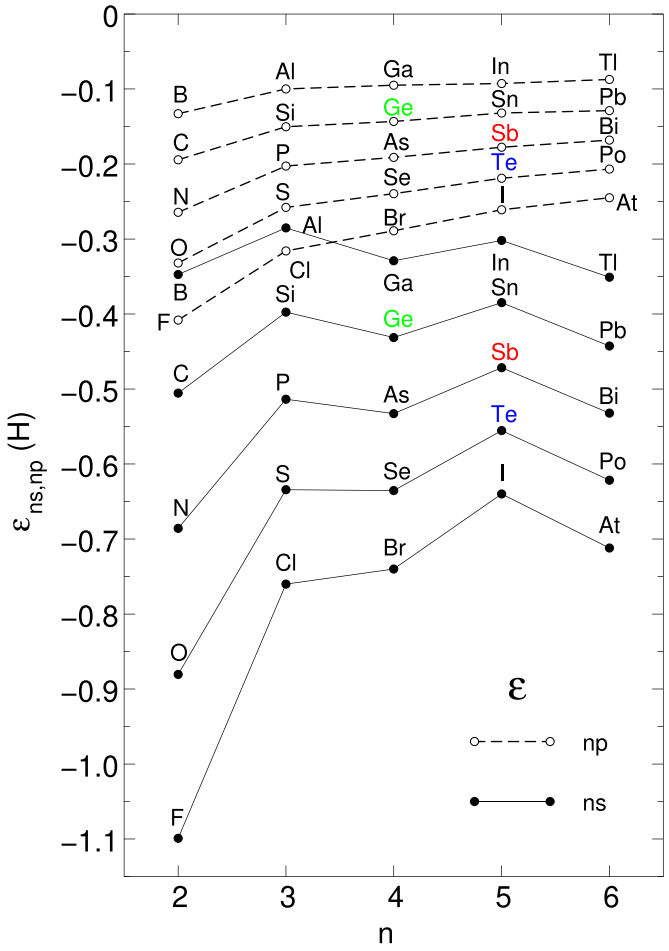

Figure 1. Eigenvalues of Kohn–Sham equations for s- (full curves) and p- (dashed curves) valence electrons in elements of the groups 13–17 (principal quantum number n from 2-6).

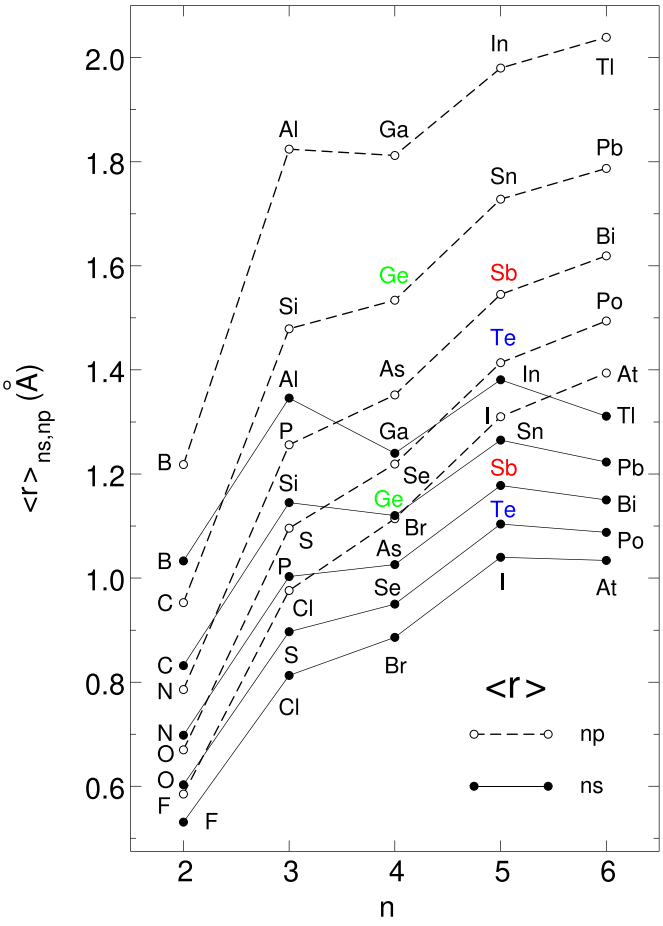

Figure 2. First radial moments (equation (1)) for s- (solid curves) and p- (dashed curves) valence electrons in elements of groups 13–17 (principal quantum number n from 2–6).

- show rapid amorphization and crystallization.
- have pronounced contrast of reflectivity or conductivity between these phases.
- be stable when operated at temperatures (100 °C–150 °C) without phase separation (segregation) or excessive power demands.

Work on PCM has been focused for almost 40 years [76] on films of alloys of Ge/Sb/Te, particularly compositions along the $(GeTe)_{1-x}(Sb_2Te_3)_x$ (GST) tieline.

3.1. Ge/Sb/Te compounds

Crystallization of GST compounds leads to a *metastable* ('FCC') form [76], and the 'key' to finding the 'ideal' PCM [77] was that it did *not* have the stable (hexagonal) layered form [78]. In fact, 'the crystalline phases in the stable state have never been used in any optical disk and electrical memory devices' [77].

In the prototype compound $Ge_2Sb_2Te_5$ (GST-225), the metastable NaCl structure was postulated to have Te atoms on one sublattice and a random mixture of Sb and Ge atoms and vacancies on the other [79]. In general, metastable GST-structures contain many vacancies and distort at room temperature for $x \leqslant 6/7$ to a rhombohedral structure [78], e.g. a GST-147 film with NaCl structure crystallizes into its stable (12-layer hexagonal) structure in several hours to several days [78].

Quenching the liquid structures results in metastable, amorphous structures containing planar 'ABAB rings' (A = Te, B = Ge, Sb) [80] and numerous other flexible structural units with bond angles near 90° and 180° [81]. The bond angle distributions in simulations of amorphous GST-225 show peaks at 90° and 170° [82–84], and show both 'ABAB rings' and pairs of such units ('ABAB cubes') [80]. Hempelmann *et al* [85] have noted the presence of 'straight atomic connectivities' in the crystalline forms. The existence of these units in both amorphous and crystalline GST-225 was postulated to promote a rapid interchange between these phases [80].

High-throughput combinatorial methods [86] based on physical vapour deposition have been used to scan properties of thin films of Ge/Sb/Te compounds [87]. These methods prepare samples spanning a continuous range of compositions, which can be studied without the need to synthesize many individual samples. The crystallization temperature T_c for

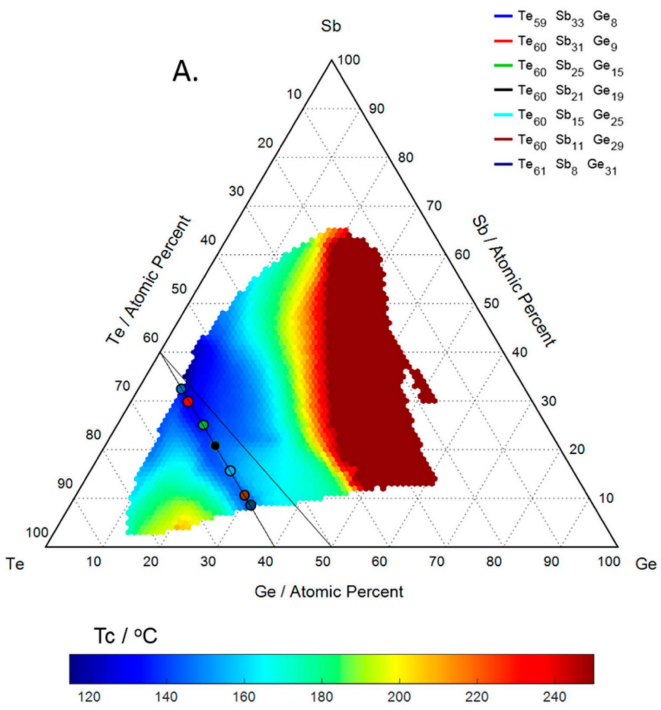

Figure 3. Compositional map of crystallization temperatures T_c of GST alloys. The black lines represent the Sb_2Te_3–GeTe and Sb_2Te_3–Ge_2Te_3 tielines. Seven compositions along the 'crystallization valley' are shown. Reprinted with permission from [87]. Copyright (2017) American Chemical Society.

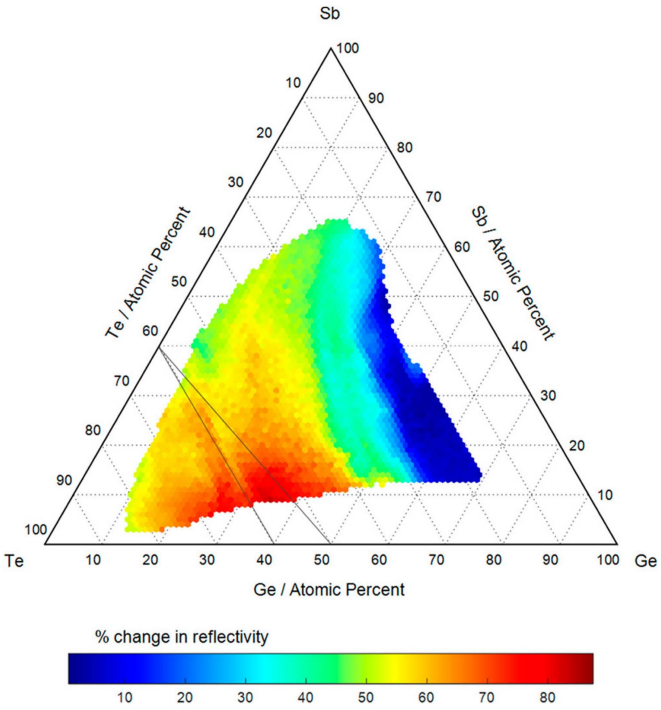

Figure 4. Compositional map of percentage change in optical reflectivity on crystallization. The black lines represent the Sb_2Te_3–GeTe and Sb_2Te_3–Ge_2Te_3 tielines. Reprinted with permission from [87]. Copyright (2017) American Chemical Society.

amorphous forms (figure 3 [87]) provides a guide to both the robustness of data storage and the power requirements for phase switching. Only small regions of the diagram provide alloys with sufficiently low T_c, and a 'crystallization valley' connecting Ge_2Te_3 with Sb_2Te_3 does *not* follow the GST tieline $(GeTe)_{1-x}(Sb_2Te_3)_x$ mentioned above. Both tielines are shown in figure 3. It is very surprising that the extensive and important structural and other information described in this work have not yet been reflected in literature citations [88].

The change in optical reflectivity on crystallization shows that adequate contrast occurs only for small regions of the Ge/Sb/Te compositional diagram (figure 4) [87], and structures determined by XRD (figure 5) show that large regions remain amorphous above 200 °C. Others segregate into mixed phases containing elemental Te, which restricts cyclability. Amorphous-to-cubic and cubic-to-hexagonal transitions can be observed near the GST tieline: cubic structures at ∼200°, the (stable) hexagonal structure at ∼300° [87]. The amorphous-to-cubic transition for these structures is typically at 140°–150°, the cubic-to-hexagonal transition at 210°–260°. In $Ge_{13}Sb_{23}Te_{64}$, for example, slightly Te-enriched from the GST-tieline, the amorphous-to-cubic phase transition was observed at 149°, the amorphous-to-hexagonal transition at 178°, and the cubic-to-hexagonal transition at 224° [87].

This information shows that compromises will always be necessary when choosing PCM: compositions near the 'GeTe-rich' end of the GST tieline have better property contrast, but

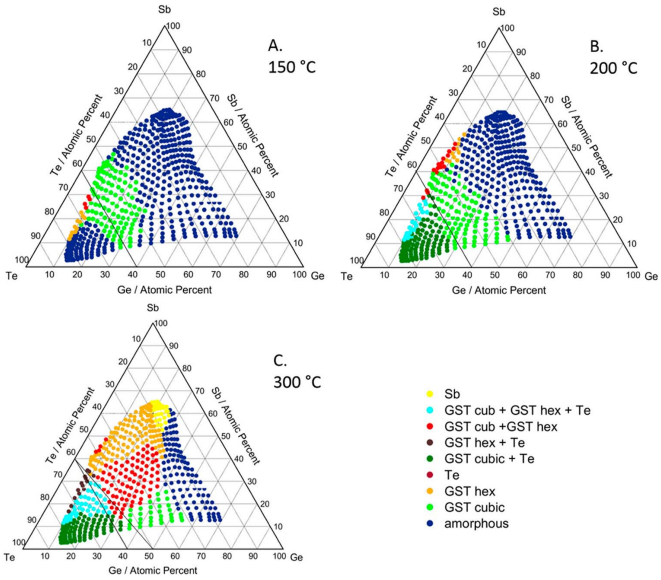

Figure 5. Compositional map of phases (or their mixtures) of Ge/Sb/Te alloys after annealing at 150 °C, 200 °C, and 300 °C. The black lines represent the Sb_2Te_3–GeTe and Sb_2Te_3–Ge_2Te_3 tielines. Reprinted with permission from [87]. Copyright (2017) American Chemical Society.

higher T_c than in Sb_2Te_3-rich compositions on either tieline. On the other hand, the amorphous phases of the latter can co-crystallize Te and not form a pure GST phase, at a temperature that can also be too low for practical PCM (figure 5). The

minimum value of T_c was found to be 115 °C for $Ge_7Sb_{36}Te_{58}$, close to 100 °C for Sb_2Te_3; T_c for GST-225 is 146.2 °C.

The identification of favourable PCM properties for Ge/Sb/Te alloys has led to many studies of other solid state solutions obtained by replacing component elements by another of the same group of the periodic table. The outcomes are sometimes surprising and difficult to predict: Partial replacement of Ge by Sn in GST-124 leads to solid solutions for all concentrations, but not for GST-225, where samples with more than 25% Sn are inhomogeneous [89]. Crystallization of films of GST-225 lead to a cubic structure, those of $Si_2Sb_2Te_5$ (SST-225) to a complex, mainly hexagonal structure [90].

3.2. Rock salt structures

In discussing the structures and properties of Ge/Sb/Te PCMs, we note first that alloys from large regions of the compositional diagram (figure 4) are quite unsuitable as PCM. There are large regions where the structure is amorphous at all temperatures considered (no 'phase change' at all), segregates into more than one phase, has a high crystallization temperature, or shows poor contrast between the properties of the phases involved. The small region of compositional space with favourable properties was identified almost 20 years ago in *structural* terms [78]: materials with metastable, rock salt structures that contain many vacancies are the first products of crystallization of the amorphous forms, not the stable, layered structures of lower energy.

Structural properties of PCM are also evident in figure 6, which maps the number of electrons shared and transferred between adjacent atomic sites some of crystalline materials [91]. Bonding mechanisms are identified and assigned colour codes, and the 'metavalent' category has been associated with favourable PCM properties. These compounds, whose structures deviate very little from octahedral coordination, crystallize rapidly:

> 'Compounds closer to the green dashed line crystallize (switch) much more rapidly than metavalent solids which are located closer to the border between metavalent and covalent bonding' [92].

There are, of course, numerous 'ionic' compounds in figure 6 with rock salt structures and much larger electron transfers.

3.3. Other structures

The critical temperature for the structural phase transition in GeTe can be manipulated in alloys with the composition $GeTe_{1-x}Sn_x$ [70], and solid solutions of GeTe-$AgSbTe_2$ show a smoothly decreasing critical temperature with increasing concentration of the second (FCC) component [93]. An extensive study of the quenched structures of high-temperature alloys of the series $(GeTe)_{1-x}Sn_xTe)_nSb_2Te_3$ [94] also showed that the structures for materials containing Sn remain closer to

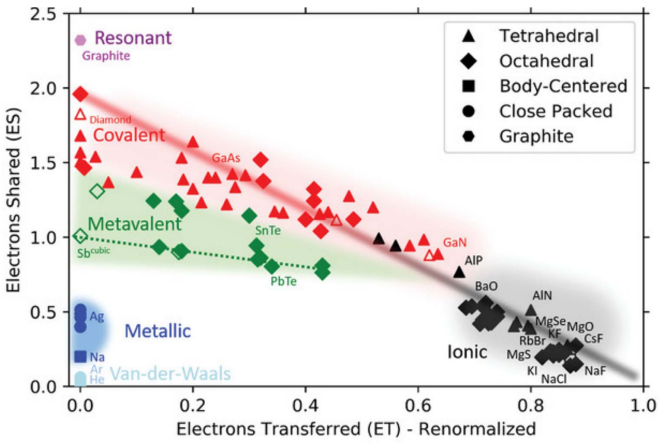

Figure 6. The number of electrons shared between adjacent atomic domains for a range of crystalline materials plotted against electron transfer (renormalized by the formal oxidation state). The bonding mechanisms as identified in [91] are shown. Triangles, diamonds, squares and circles denote tetrahedrally, distorted and ideal rocksalt (octahedrally coordinated), and close-packed metallic structures. The dotted green line connects perfectly octahedral structures. [91] John Wiley & Sons. [© 2020 The Authors. Published by WILEY-VCH Verlag GmbH & Co. KGaA, Weinheim].

cubic, the phase transitions occur at significantly lower temperatures, and the higher electrical conductivities (compared with the corresponding GST material) lead to better thermoelectric figures of merit. A similar improvement is found in the cubic phase of SnSe obtained from the *Pnma* (orthorhombic) form by alloying with $AgSbTe_2$ and related compounds [95]. These are examples of the structural transitions occurring in compounds of elements of groups 14 and 16 and of ways that structures and the related functions can be optimized. Furthermore, the rock salt structures in PbS, PbTe, and SnTe can be transformed into *Pnma* structures under high pressure, and epitaxial growth on rock salt of normally *Pnma* structures of SnS and SnSe induce rock salt structures [96].

4. Discussion

If we include vacancies as 'atomic sites', the average VEC per site of GST alloys near the GST-tieline is close to five ($\langle \mathbf{5} \rangle$, approximately two s-electrons, three p-electrons). We can then adopt the NFE arguments of Jones [62] (section 2.7) that explained the structure and properties of bismuth and other group 15 elements. This model is three-dimensional, unlike the one-dimensional model of Peierls [64], where it is necessary to '... make the simplifying assumption that we can treat the p_x, p_y, and p_z orbitals independently, so that the cubic structure can be treated as independent, one-dimensional chains [53, p 243]'. Cohen *et al* [69] showed that NFE arguments also apply to 14–16 compounds, provided that the 'chemical difference between the 14 and 16 components' is small, as in GeTe. In this case, a small rhombohedral distortion of the octahedral structure will result. Large antisymmetric components

of the pseudopotential [69] lead to insulators with rock salt structures.

The moments of the valence orbitals in Ge, Sb, Te, and—to a lesser extent—Sn are remarkably similar (figure 2), as are the Pauling electronegativities (2.01, 2.05, 2.1, 1.96, respectively). Nevertheless, the structures must also reflect the pronounced differences between the VEC (Ge $3s^2 3p^2$, Sb $4s^2 4p^3$, Te $4s^2 4p^4$, vacancies $s^0 p^0$). An average configuration with five valence electrons can be maintained if Sb and, particularly, Ge atoms move away from vacancies and accumulate near Te atoms. Precisely these trends are observed in density functional simulations of GST-225 [97, 98], where very few vacancies have Ge or Sb atoms as neighbours in the ordered, metastable structure.

The Ge/Sb/Te alloys with properties appropriate for PCMs are confined to a small region of the compositional structure diagram (figure 5) that includes the pseudobinary tieline GeTe–Sb_2Te_3. Apart from GeTe, Te ($5s^2 5p^4$) makes up more than half of the atoms for these compositions, the p-shell is more than half full, and the Lewis octet rule (each atom is associated with four electron pairs) will not be satisfied. Covalent bonds occur, but non-bonding valence electron orbitals ('lone pairs') are also occupied. This leads to electron-rich, multicentre ('hypervalent' [99]) bonds, the '… natural extension of covalent electron-pair bonding to electron-deficient or electron-rich systems' [44, p 2414].

The electronic configuration $s^2 p^3$ with three orthogonal p-orbitals is often associated with cubic (e.g. [69]) or 'pseudocubic' structures [94]. Nevertheless, non-cubic structures occur often in clusters and disordered systems with half-filled p-shells. The bond angle distributions in liquid Sb [100] and Bi [101] show prominent peaks near 90°, but also peaks near 60° and 140°. The most stable crystalline form of phosphorus (black P, orthorhombic) can be converted under pressure successively to rhombohedral (A7) and SC structures [102, 103], and the A7 structures of the remaining group 15 elements convert under pressure to SC [102, 104, 105]. Density functional calculations show that the cubic (O_h) structures of the clusters P_8 [106], As_8 [107], Sb_8 [100], and Bi_8 [101] are substantially less stable than the wedge-shaped (C_{2v}, cuneane) isomers, which have bond angles near 60° and 120°, *and* 90°, although the energy differences decrease with increasing atomic number from over 1.7 eV in P_8 to less than 0.5 eV in Bi_8.

Disordered forms of PCM crystallize to *metastable* structures, not the stable crystalline form of the material. According to the Ostwald *Stufensatz* ('step rule', [108]), as extended by Stranski and Totomanov [109], the first stage of nucleation is to the metastable form separated from the initial state by the smallest free energy barrier. On the basis of irreversible thermodynamics, van Santen [110] showed that multiple step reactions via metastable structures ('successive transformations') lead to a lower entropy production than in the direct reaction, i.e. the *multiple* nature of the indirect process is crucial in these systems, not the rate of the direct process.

5. Concluding remarks

An Internet search for 'structure/function relationship' shows a distinct bias towards biology, and the focus on protein structures in the award of the 2024 Nobel Prize in Chemistry confirms its importance in this area. The examples given in section 2 underline, however, the importance of geometric structure in chemistry and condensed matter physics. This is self-evident in structural phase changes, and the example we have discussed covers the structures (section 3) of PCMs, particularly Ge/Sb/Te alloys.

In the context of PCM crystallization, it has been observed [111] that:

> 'These findings provide two guidelines on how to identify materials with ultra-fast crystallization. We can either experimentally search for compounds with octahedral-like atomic arrangement, yet small distortions and an average of 3 p-electrons per atom, or perform quantum chemical calculations and search for compounds with near-perfect octahedral arrangement, which share about 1 electron between adjacent atoms.'

Seeking to minimize deviations from octahedral coordination supports our emphasis on *structure*, and the extensive structural information already available for a library of Ge/Sb/Te compounds [87] should make unnecessary the large number of quantum chemical calculations advocated in the second option.

The structures have indeed provided insight and *understanding* of PCM properties, as suggested in the title, even if their actual derivation is often more complicated. Commercial PCM almost always have rock salt structures, and we have noted that GST compounds, in particular, have an average of five sp- valence electrons per atom and component orbitals of similar extent. The simple picture of Jones [62] explains the existence of rock salt structures that are less stable than the layered crystalline formss.

It has also been proposed [112] that the particular 'property portfolio' of PCM is due to a common, 'unique' bonding mechanism. It would be very welcome if *correlations* between known properties could aid the development of materials with favourable values of other properties, but a simple example shows that identifying a *causal* relationship between correlated quantities can be difficult.

There is a statistically significant correlation ($p = 0.008$) between the number of human births and the number of nesting pairs of storks in 17 European countries between 1980 and 1990 (figure 7(a) [113]). This means that there is only 1 chance in 125 of obtaining at least as good a correlation with a dataset where no correlation is assumed. The very low p-value implies a strong correlation, but it does *not* imply that the hypothesis is true, even for $p = 0$.

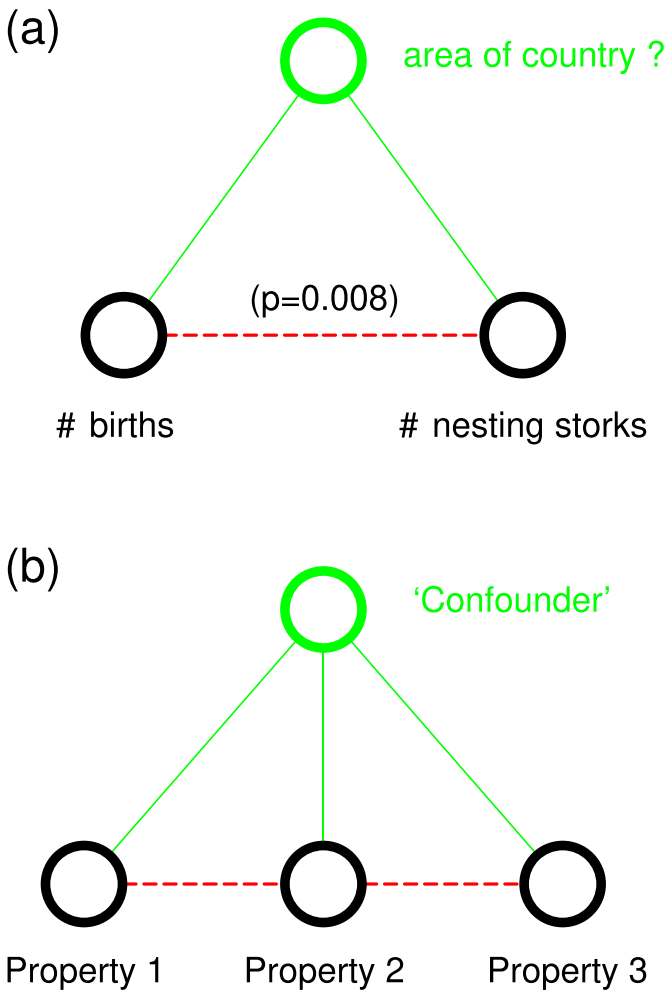

Figure 7. Correlation, not causation. (a) There is a statistically significant correlation ($p = 0.008$) between the number of human births in 17 European countries (1980–1990) and the number of nesting storks [113]. (b) Correlations between different properties may arise when *both* properties correlate separately with the same 'confounder'.

It is highly unlikely that these measured quantities are linked in a causal way, but there may be a confounding variable (the land area of the country in this case) that is common to both variables (figure 7(b)) and leads to a non-trivial, statistically significant correlation between them. The possible existence of 'confounders' must be considered before drawing conclusions based on such correlations, and the structure of a system should be a better choice of 'confounder' (figure 7(b)) than the bonding mechanism assigned to it.

Data availability statement

No new data were created or analyzed in this study.

Acknowledgments

I thank R Dronskowski for numerous helpful suggestions, particularly concerning the chemical literature.

ORCID iD

R O Jones https://orcid.org/0000-0003-1167-4812

References

[1] Crick F 1990 *What Mad Pursuit: A Personal View of Scientific Discovery* (Penguin)
[2] Press release, Royal Swedish Academy of Sciences, Stockholm, 9 October 2024 (available at: https://.nobelprize.org/prizes/chemistry/2024/press-conference)
[3] Pauling L 1960 *The Nature of the Chemical Bond and the Structure of Molecules and Solids* 3rd edn (Cornell University Press)
[4] Pauling L 1929 *J. Am. Chem. Soc.* **51** 1010–26
[5] Pearson W B 1972 *The Crystal Chemistry and Physics of Metals and Alloys* (Wiley)
[6] Goldschmidt V M 1926 *Naturwissenschaften* **14** 477–85
[7] Hume-Rothery W 1973 *J. Inst. Met.* **35** 295–361
[8] Hume-Rothery W and Raynor G V 1962 *The Structure of Metals and Alloys* 4th (revised) edn (The Institute of Metals)
[9] Jones R O 2024 *Solid State Sci.* **152** 107524
[10] Jones R O 2018 *J. Phys.: Condens. Matter* **30** 153001
[11] Frankland E 1866 *Lecture Notes for Chemical Students* (John van Voorst)
[12] Frankland E 1866 *J. Chem. Soc.* **19** 372–95
[13] Jones R O 2022 *J. Phys.: Condens. Matter* **34** 343001
[14] Müller U 2006 *Inorganic Structural Chemistry* 2nd edn (Wiley)
[15] Burdett J K 1995 *Chemical Bonding in Solids* (Oxford University Press) (available at: https://books.google.de/books?id=s5-2QgAACAAJ)
[16] Berger R F, Walters P L, Lee S and Hoffmann R 2011 *Chem. Rev.* **111** 4522–45
[17] Wuttig M, Schön C-F, Kim D, Golub P, Gatti C, Raty J-Y, Kooi B J, Pendás A M, Arora R and Waghmare U 2024 *Adv. Sci.* **11** 2308578
[18] Jones R O, Elliott S R and Dronskowski R 2023 *Adv. Mater.* **35** 2300836
[19] Müller P C, Elliott S R, Dronskowski R and Jones R O 2024 *J. Phys.: Condens. Matter* **36** 325706
[20] Aste T and Weaire D 2000 *The Pursuit of Perfect Packing* (Institute of Physics Publishing)
[21] Goldschmidt V M 1927 *Ber. Dtsch. Chem. Ges.* **60** 1263–96
[22] Pauling L 1927 *J. Am. Chem. Soc.* **49** 765–90
[23] Pauling L 1928 *Z. Kristallogr.* **67** 377–404
[24] Zachariasen W H 1931 *Z. Kristallogr.* **80** 137–53
[25] Ladd M F C 1968 *Theor. Chim. Acta* **12** 333–6
[26] Shannon R D and Prewitt C T 1970 *J. Inorg. Nucl. Chem.* **32** 1427–41
[27] Shannon R D 1976 *Acta Crystallogr.* A **32** 751–67
[28] George J, Waroquiers D, Di Stefano D, Petretto G, Rignanese G-M and Hautier G 2020 *Angew. Chem., Int. Ed.* **59** 7569–75
[29] Laves F 1930 *Z. Kristallogr.* **73** 202–65
[30] Laves F 1930 *Z. Kristallogr.* **73** 275–324
[31] Laves F and Witte H 1935 *Metallwirtschaft* **14** 645–9
[32] Laves F and Witte H 1936 *Metallwirtschaft* **15** 840–2
[33] Murray M J and Sanders J V 1980 *Phil. Mag.* A **42** 721–40
[34] Simon A 1983 *Angew. Chem., Int. Ed.* **22** 95–113
[35] Stein F and Leineweber A 2021 *J. Mater. Sci.* **56** 5321–427
[36] Ormeci A, Simon A and Grin Y 2010 *Angew. Chem., Int. Ed.* **49** 8997–9001
[37] Laves F 1956 Crystal structure and atomic size *Theory of Alloy Phases* (American Society for Metals) pp 124–98 (available at: https://books.google.de/books?id=mj8cvwEACAAJ)

[38] Parthé E 1961 *Z. Kristallogr. - Cryst. Mater.* **115** 52–79
[39] Zintl E 1939 *Angew. Chem.* **52** 1–6
[40] Laves F 1941 *Naturwissenschaften* **29** 244–55
[41] Klemm W 1958 *Proc. Chem. Soc.* 329–41
[42] Schäfer H, Eisenmann B and Müller W 1973 *Angew. Chem., Int. Ed.* **12** 694–712
[43] Nesper R 2014 *Z. Anorg. Allgem. Chem.* **640** 2639–48
[44] Papoian G A and Hoffmann R 2000 *Angew. Chem., Int. Ed.* **39** 2408–48
[45] Mott N F and Jones H 1936 *The Theory of the Properties of Metals and Alloys* (Clarendon)
[46] Jones H 1937 *Proc. Phys. Soc.* **49** 250–7
[47] Jones H 1975 *The Theory of Brillouin Zones and Electronic States in Crystals* 2nd revised edn (North-Holland)
[48] Evans R, Lloyd P and Mujibur R 1979 *J. Phys. F: Met. Phys.* **9** 1939
[49] Paxton A T, Methfessel M and Pettifor D G 1997 *Proc. R. Soc.* A **453** 1493–514
[50] Mizutani U, Sato H and Massalski T 2021 *Prog. Mater. Sci.* **120** 100719
[51] Hoppe R 1970 *Angew. Chem., Int. Ed.* **9** 25–34
[52] Grimm H G 1934 *Angew. Chem.* **47** 53–58
[53] Littlewood P B 1983 *Crit. Rev. Solid State Mater. Sci.* **11** 229–85
[54] St John J and Bloch A N 1974 *Phys. Rev. Lett.* **33** 1095–8
[55] Watson R E and Bennett L H 1978 *Phys. Rev.* B **18** 6439–49
[56] Zunger A 1980 *Phys. Rev.* B **22** 5839–72
[57] Machlin E S and Loh B 1980 *Phys. Rev. Lett.* **45** 1642–4
[58] Pettifor D 1984 *Solid State Commun.* **51** 31–34
[59] Pettifor D G 1992 Structure maps for ordered intermetallics *Ordered Intermetallics—Physical Metallurgy and Mechanical Behaviour* ed C T Liu, R W Cahn and G Sauthoff (Springer) pp 47–59 (https://doi.org/10.1007/978-94-011-2534-5_4)
[60] Mooser E and Pearson W B 1959 *Acta Crystallogr.* **12** 1015–22
[61] Peierls R 1930 *Ann. Phys., Lpz.* **396** 121–48
[62] Jones H 1934 *Proc. R. Soc.* A **147** 396–417
[63] Jones R O 2020 *Phys. Rev.* B **101** 024103
[64] Peierls R E 1955 *Quantum Theory of Solids* (Clarendon)
[65] Friedel J 1992 *Phil. Mag.* B **65** 1125–9
[66] Shick A B, Ketterson J B, Novikov D L and Freeman A J 1999 *Phys. Rev.* B **60** 15484–7
[67] Heine V and Jones R O 1969 *J. Phys. C: Solid State Phys.* **2** 719–32
[68] Schiferl D 1974 *Phys. Rev.* B **10** 3316–29
[69] Cohen M H, Falicov L M and Golin S 1964 *IBM J.* **8** 215–27
[70] Bierly J N, Muldawer L and Beckman O 1963 *Acta Metall. Mater.* **11** 447–54
[71] Biron E V 1915 *Zh. Russ. Fiz.-Khim. Obshch.* **47** 964–88
[72] Pauling L 1932 *J. Am. Chem. Soc.* **54** 3570–82
[73] Mulliken R S 1934 *J. Chem. Phys.* **2** 782–93
[74] Denton A R and Ashcroft N W 1991 *Phys. Rev.* A **43** 3161–4
[75] Vegard L 1921 *Z. Phys.* **5** 17–26
[76] Yamada N, Ohno E, Akahira N, Nishiuchi K, Nagata K and Takao M 1987 *Jpn. J. Appl. Phys.* **26** 61–66
[77] Yamada N 2012 *Phys. Status Solidi* b **249** 1837–42
[78] Matsunaga T, Kojima R, Yamada N, Kifune K, Kubota Y, Tabata Y and Takata M 2006 *Inorg. Chem.* **45** 2235–41
[79] Yamada N 1996 *MRS Bull.* **21** 48–50
[80] Akola J and Jones R O 2007 *Phys. Rev.* B **76** 235201
[81] Lee T H and Elliott S R 2017 *Adv. Mater.* **29** 1700814
[82] Akola J and Jones R O 2008 *J. Phys.: Condens. Matter* **20** 465103
[83] Mocanu F C, Konstantinou K, Lee T H, Bernstein N, Deringer V L, Csányi G and Elliott S R 2018 *J. Phys. Chem.* B **122** 8998–9006
[84] Abou El Kheir O, Bonati L, Parrinello M and Bernasconi M 2024 *npj Comput. Mater.* **10** 33
[85] Hempelmann J, Müller P C, Ertural C and Dronskowski R 2022 *Angew. Chem., Int. Ed.* **61** e202115778
[86] Gebhardt T, Music D, Takahashi T and Schneider J M 2012 *Thin Solid Films* **520** 5491–9
[87] Guerin S, Hayden B, Hewak D W and Vian C 2017 *ACS Comb. Sci.* **19** 478–91
[88] In the seven years to 1 August 2024, the article had been cited less than 40 times on Clarivate WebofScience.
[89] Welzmiller S, Rosenthal T, Ganter P, Neudert L, Fahrnbauer F, Urban P, Stiewe C, de Boor J and Oeckler O 2014 *Dalton Trans.* **43** 10529–40
[90] Zhang T, Cheng Y, Song Z, Liu B, Feng S, Han X, Zhang Z and Chen B 2008 *Scr. Mater.* **58** 977–80
[91] Kooi B J and Wuttig M 2020 *Adv. Mater.* **32** 1908302
[92] Raty J-Y, Bichara C, Schön C-F, Gatti C and Wuttig M 2024 *Proc. Natl Acad. Sci. USA* **121** e2316498121
[93] Baleva M I and Plachkova S K 1983 *J. Phys. C: Solid State Phys.* **16** 791
[94] Rosenthal T, Neudert L, Ganter P, de Boor J, Stiewe C and Oeckler O 2014 *J. Solid State Chem.* **215** 231–40
[95] Lin N *et al* 2024 *Adv. Funct. Mater.* **34** 2315652
[96] Mariano A N and Chopra K L 1967 *Appl. Phys. Lett.* **10** 282–4
[97] Kalikka J, Akola J and Jones R O 2014 *Phys. Rev.* B **90** 184109
[98] Kalikka J, Akola J and Jones R O 2016 *Phys. Rev.* B **94** 134105
[99] Lee T H and Elliott S R 2022 *Nat. Commun.* **13** 1458
[100] Jones R O, Ahlstedt O, Akola J and Ropo M 2017 *J. Chem. Phys.* **146** 194502
[101] Akola J, Atodiresei N, Kalikka J, Larrucea J and Jones R O 2014 *J. Chem. Phys.* **141** 194503
[102] Donohue J 1974 *The Structures of the Elements* (Wiley)
[103] Sasaki T, Shindo K, Niizeki K and Morita A 1988 *J. Phys. Soc. Japan* **57** 978–87
[104] Kikegawa T and Iwasaki H 1987 *J. Phys. Soc. Japan* **56** 3417–20
[105] Ono S 2018 *High Press. Res.* **38** 414–21
[106] Jones R O and Hohl D 1990 *J. Chem. Phys.* **92** 6710–21
[107] Ballone P and Jones R O 1994 *J. Chem. Phys.* **100** 4941–6
[108] Ostwald W 1897 *Z. Phys. Chem.* **22U** 289–330
[109] Stranski I N and Totomanow D 1933 *Z. Phys. Chem.* **163A** 399–408
[110] van Santen R A 1984 *J. Phys. Chem.* **88** 5768–9
[111] Persch C *et al* 2021 *Nat. Commun.* **12** 4978
[112] Wuttig M, Schön C-F, Lötfering J, Golub P, Gatti C and Raty J-Y 2023 *Adv. Mater.* **35** 2208485
[113] Matthews R 2000 *Teach. Stat.* **22** 36–38